Microstrip Circuit Applications of High-Q Open Microwave Resonators

KARL D. STEPHAN, MEMBER, IEEE, SONG-LIN YOUNG, AND SAI-CHU WONG

Abstract—**The problem of achieving a high circuit Q in hybrid and monolithic microwave integrated circuits becomes acute in the millimeter-wave range. An open microwave resonator can be formed above a planar microstrip substrate by suspending a spherical reflector above it. We develop a theory to account for the coupling between an open resonator mode and a microstrip line. The open resonator is shown to have useful circuit properties similar to a dielectric resonator, but with the potential of efficient operation well into the millimeter wave range. Experimental confirmation of the theory is demonstrated by a scale model of a microstrip-based single-pole bandpass filter, which shows a loaded Q of 860 and a minimum loss of 0.8 dB $\pm$ 0.4 dB at 10 GHz.**

I. Introduction

HYBRID AND MONOLITHIC microwave integrated circuits (MIC's) can now perform nearly all microwave circuit functions that were formerly realized with classical waveguide or coaxial designs. However, applications requiring a circuit element Q greater than about 300 have resisted efforts at integration because of the intrinsic limitations of planar transmission-line media [1]. Although the use of dielectric resonators can alleviate this problem, at millimeter wavelengths these devices become very small and difficult to mount repeatably. Thus, narrow percentage bandwidth filters, high-power combiners, and other components that are intolerant of circuit losses have not been possible up to now in MIC design. Even conventional waveguide–cavity resonators show degraded performance above 30 GHz, leaving the millimeter wave circuit designer with very few options for achieving high Q circuit functions.

By utilizing the free space above a microstrip circuit for energy storage, we have found that circuit Q's above the generally accepted limits for microstrip elements can be achieved in a quasiplanar configuration. We form an open resonator by suspending a spherical reflector above a microstrip line. Such an open cavity supports fewer modes than a conventional closed cavity of similar dimensions. (In a practical circuit enclosure the resonator periphery can be lined with absorbing material.) The modes sustained within the resonator typically have unloaded Q values on the order of 10^5 for reasonable cavity dimensions. When a microstrip line is coupled to such an open resonator mode, the energy stored in the resonator volume becomes accessible to the microstrip circuit, resulting in loaded Q's of several hundred to several thousand. In this paper, we develop a theory which leads to simple lumped equivalent circuits for the coupling mechanisms between the open resonator and microstrip. Experiments are presented and compared with the predictions of the theory. Finally, some applications of this technique are discussed, including filters, oscillators, and power combiners.

Manuscript received October 3, 1987; revised April 27, 1988. This work was supported by the U.S. Army Research Office under Contract DAAL03-86-K-0087.

The authors are with the Department of Electrical and Computer Engineering, University of Massachusetts, Amherst, MA 01003.

IEEE Log Number 8822321.

II. Theory

A. Empty Resonator

Since the empty open resonator consisting of one flat and one concave spherical mirror is the same type of modified Fabry–Perot structure used in many lasers, it has been studied extensively by numerous authors [2], [3]. Mink [4] analyzed the fields inside such a quasi-optical resonator in connection with power combining of solid state millimeter wave sources. At millimeter wavelengths, the geometric–optics assumption that the wavelength is negligibly small compared to the cavity dimensions is no longer valid and diffraction effects become increasingly significant. Cullen [5] has summarized the best current theoretical models for fields inside a millimeter wave open resonator of practical dimensions. For the purposes of our analysis a scalar-field approach gives satisfactory precision, and it is this approach as presented by Cullen that we will now review.

Fig. 1 illustrates an open resonator formed when a flat reflector at $z = 0$ faces a spherical concave reflector of radius R_0 at $z = D$. The solution of interest results from equating the scalar-field variable to the y-directed magnetic field, assuming that the radial-field dependence is much slower than the variation along the resonator z axis, and solving the resulting scalar Helmholtz equation. The result is in terms of the y-directed magnetic field:

$$H_y = H_0 \frac{w_0}{w(z)} \cos\left[kz - \Phi(z) + k\rho^2/2R(z)\right] \cdot \exp\left[-\rho^2/w^2(z)\right]. \quad (1)$$

In addition to the free-space wavenumber $k = 2\pi/\lambda$ and radial distance from the axis $\rho = \sqrt{x^2 + y^2}$, the special

0018-9480/88/0900-1319$01.00 ©1988 IEEE

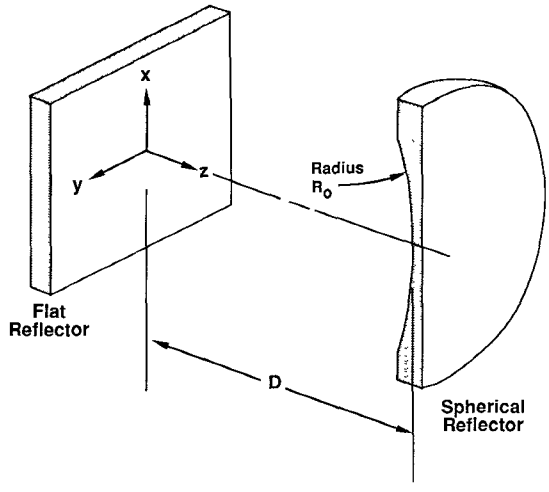

Fig. 1. Empty open-cavity microwave resonator.

functions

$$\Phi(z) = \arctan(z/z_0) \tag{2}$$

$$R(z) = z\left(1 + z_0^2/z^2\right) \tag{3}$$

$$w^2(z) = \frac{\lambda z_0}{\pi}\left(1 + z^2/z_0^2\right) \tag{4}$$

are defined in terms of a characteristic length z_o which will shortly be determined from the boundary conditions. The field described by (1) is a standing wave, approximately plane near the flat reflector, whose amplitude shows a Gaussian dependence on radius ρ. Thus it is termed a Gaussian beam. At $z = 0$ the radius, measured from the resonator axis, at which the amplitude falls to $1/e$ of its on-axis value is termed the beam radius or scale radius w_0, which is related to the characteristic length z_0 by

$$w_0^2 = \frac{\lambda z_0}{\pi}. \tag{5}$$

The electric field coexisting with the magnetic field of (1) is

$$E_x = -jH_0\left[\frac{\mu_0}{\epsilon_0}\right]^{1/2}\frac{w_0}{w(z)}\sin\left[kz - \Phi(z) + k\rho^2/2R(z)\right] \cdot\exp\left[-\rho^2/w^2(z)\right] \tag{6}$$

where μ_0 and ϵ_0 are the permeability and permittivity of vacuum, respectively.

To determine z_0 we require tangential E to vanish on the surface of the spherical reflector, which intersects the z axis at $z = D$. Near the z axis $E_{\tan} \approx E_x$ and, recognizing that $R(z)$ is the radius of curvature of the phase front, we use (3) to find that

$$z_0 = \sqrt{D(R_0 - D)}. \tag{7}$$

The boundary conditions will be satisfied only for certain values of $k = \kappa_q$ corresponding to the TEM_{00q} modes of the empty resonator. It can be shown that

$$\kappa_q = \frac{(q+1)\pi + \arctan\left[\sqrt{D/(R_0 - D)}\right]}{D}. \tag{8}$$

This completes the analysis of the empty resonator.

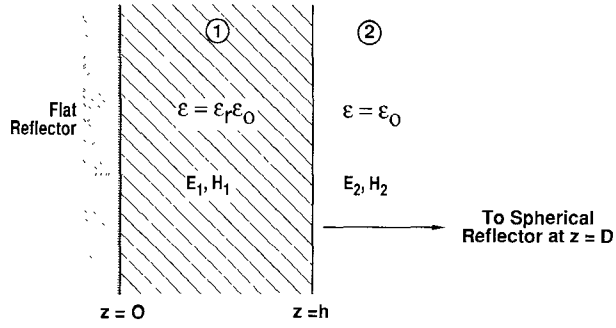

Fig. 2. Fields near a flat reflector which supports a dielectric substrate of thickness h.

B. Resonator with Dielectric Substrate

Suppose that the flat reflector now supports an electrically thin dielectric substrate as shown in Fig. 2. To be suitable for microstrip service the substrate height h must be no thicker than approximately

$$h_{\max} = \frac{1}{10}\frac{\lambda}{\sqrt{\epsilon_r}} \tag{9}$$

where ϵ_r is the dielectric constant of the substrate relative to vacuum and λ is the free-space wavelength. This limitation permits considerable simplification of the analysis. At the surface of this thin dielectric, the fields are essentially plane waves with a Gaussian dependence on radius. This assumption allows the replacement of the dielectric slab of thickness h with an electrically equivalent empty space of thickness t, given by

$$t = \frac{1}{k}\arctan\left[\frac{\tan\left(kh\sqrt{\epsilon_r}\right)}{\sqrt{\epsilon_r}}\right]. \tag{10}$$

In order to keep a similar form for the fields near the ground plane for the empty resonator case and the resonator with dielectric, we make the substitution $z' = z + (t - h)$ into (1) and (6) to find the fields within the dielectric of region 1, bearing in mind that the relative permittivity of the dielectric is ϵ_r. Matching boundary conditions ($E_{x_1} = E_{x_2}$ and $H_{y_1} = H_{y_2}$ at $z = h$) yields expressions for the fields E_{x_2} and H_{y_2} in region 2. With the added condition that the beam radius w_0 equals or exceeds λ, it can be shown that the following expressions agree with the more exact analysis of Cullen [5] to within 2° of the harmonic function arguments and one percent of the true beam radius:

Region 1 ($0 < z \leqslant h$):

$$H_{y1} = H_0\cos(k_d z)\exp\left(-\rho^2/w_0^2\right) \tag{11}$$

$$E_{x1} = -j\frac{H_0}{\sqrt{\epsilon_r}}\left[\frac{\mu_0}{\epsilon_0}\right]^{1/2}\sin(k_d z)\exp\left(-\rho^2/w_0^2\right). \tag{12}$$

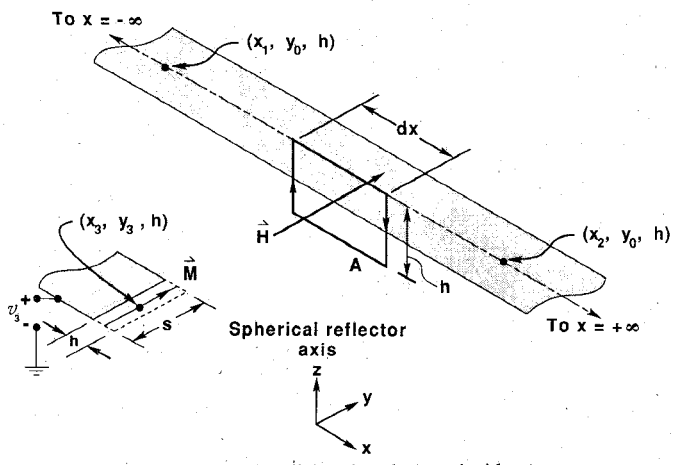

Fig. 3. Microstrip lines on dielectric substrate inside open resonator.

Region 2 ($h < z < D$):

$$H_{y2} = H_0 \frac{w_0}{w(z')} \frac{\cos(k_d h)}{\cos(kt)} \cos\left[kz' - \Phi(z') + k\rho^2/2R(z')\right] \cdot \exp\left[-\rho^2/w^2(z')\right] \tag{13}$$

$$E_{x2} = \frac{-jH_0}{\sqrt{\epsilon_r}} \left[\frac{\mu_0}{\epsilon_0}\right]^{1/2} \frac{w_0}{w(z')} \frac{\sin(k_d h)}{\sin(kt)} \cdot \sin\left[kz' - \Phi(z') + k\rho^2/2R(z')\right] \exp\left[-\rho^2/w^2(z')\right] \tag{14}$$

where $k_d = k\sqrt{\epsilon_r}$ is the wavenumber in the dielectric and the substrate permeability μ_0 is assumed to be that of vacuum. The expressions for the characteristic length z_0 and resonant wavenumber κ_q must now be modified to

$$z_0' = \sqrt{(D + t - h)(R_0 + D + t - h)} \tag{15}$$

and

$$\kappa_q' = \frac{(q+1)\pi + \arctan\left[\sqrt{(D + t - h)/(R_0 - D - t + h)}\right]}{D + t - h}. \tag{16}$$

Since the substrate is near an electric field minimum, these corrected values for characteristic length and resonant wavenumber are usually within one percent or less of the corresponding unprimed empty resonator figures, which may consequently be used without serious error.

C. Resonator with Magnetic Current Source and Microstrip Line

In Fig. 3 we show two microstrip lines on the surface of the dielectric substrate of subsection B. The microstrip line in the upper part of the figure extends from $x = -\infty$ to $x = +\infty$ along its axis $y = y_0$. The second microstrip line terminates in an open circuit at $(x_3 - h/2,\ y_3,\ h)$ where an ac voltage v_3 is maintained at the open end with respect to the ground plane. Following Derneryd [6], we replace the second microstrip by a magnetic current element of magnitude $M_y = v_3/h$, oriented as shown.

This magnetic current excites fields in the open cavity resonator which can be expressed exactly, in principle, as an infinite sum of the various orthogonal cavity-mode fields. Since the TEM_{00q} modes have very high Q values, only one mode is excited significantly near a given resonant frequency, and the terms in the expansion corresponding to the other modes are comparatively small. An analysis that approximates the total field by a single term in the expansion will accurately model the coupling mediated by the mode corresponding to that term near its resonant frequency, and this is the path we will pursue.

Using a single term in the expansion, we obtain this expression for the cavity's magnetic field $\vec{H}$ [7]:

$$\vec{H} = \vec{H}_0 \left(\frac{j\omega}{\omega^2 - \omega_0^2}\right) \iiint_V \vec{M} \cdot \vec{H}_0^* \, d\tau \tag{17}$$

in which ω_0 is the mode's complex resonant frequency. The mode field $\vec{H}_0$ must be normalized so that integration over the cavity volume V yields

$$\mu_0 \iiint_V \vec{H}_0 \cdot \vec{H}_0^* \, d\tau = 1. \tag{18}$$

Imposing this normalization condition leads to a value for H_0 in (1) of $H_0 = (2/w_0)(\pi G \mu_0)^{-1/2}$, in which G is a length related to the inter-reflector distance D by

$$G = \frac{\cos^2(k_d h)}{\cos^2(kt)} \left[D - h - \frac{\sin(2kt)}{k}\right] + h + \frac{\sin(2k_d h)}{k_d}. \tag{19}$$

For the equivalent magnetic current of Fig. 3, the integration of (17) yields a relation between the cavity field $\vec{H}$ and the voltage v_3:

$$\vec{H} = \vec{H}_0 \left(\frac{j\omega}{\omega^2 - \omega_0^2}\right) \left[sH_0 \cos(k_d h) \exp\left(-\rho_3^2/w_0^2\right)\right] v_3 \tag{20}$$

in which $\rho_3^2 = x_3^2 + y_3^2$ and s is the microstrip width. In this expression the value of the magnetic field over the relatively small magnetic current area has been approximated as a constant equal to its value at (x_3, y_3, h).

We next assume that the presence of the infinite microstrip line leaves the magnetic field of (20) undisturbed to first order. Since the electrically thin substrate places the microstrip near the electric-field null at $z = 0$, this assumption is reasonable. Considering the contour A in Fig. 3 as being centered beneath the infinite microstrip, Faraday's law gives

$$\oint_A \vec{E} \cdot d\vec{l} = -j\omega\mu_0 \iint_A \vec{H} \cdot d\vec{a}. \tag{21}$$

Since the top and bottom segments of A lie on conductors, only the vertical segments along E_z contribute to the left-hand side of (21), which can be expressed in terms of a differential induced voltage:

$$\delta(x) = h\left[E_z(x + dx) - E_z(x)\right] = -\oint_A \vec{E} \cdot d\vec{l}. \tag{22}$$

When this term is added to the telegrapher's equation for

voltage and current along a transmission line having inductance L and capacitance C per unit length, we obtain this differential equation for the microstrip line voltage $v(x)$:

$$\frac{d^2v}{dx^2} - \frac{d}{dx}\left[\frac{\delta(x)}{dx}\right] = -\omega^2 LCv. \tag{23}$$

The induced voltage derivative $\delta(x)/dx$ can be found by substituting (20) into (21) and using (22) to find that

$$\frac{\delta(x)}{dx} = v_3 F(\omega)\exp\left(-x^2/\omega_0^2\right) \tag{24}$$

in which the function of frequency $F(\omega)$ is defined as

$$F(\omega) = \frac{-\omega^2}{\left(\omega^2-\omega_0^2\right)}\frac{4sh}{\pi w_0^2 G}\cos(k_d h)\frac{\sin(k_d h)}{k_d h} \cdot\exp\left(-y_0^2/w_0^2\right)\exp\left(-\rho_3^2/w_0^2\right). \tag{25}$$

A solution of (23), with the exponential function of x in (24) substituted for $\delta(x)$, can be found by Fourier-transform methods [8]. The inhomogeneous solution induced by the driving voltage v_3 is found to be

$$\begin{aligned} v(x) = {} & \frac{v_3 F w_0\sqrt{\pi}}{2}\cdot e^{-x^2/\omega_0^2} \\ & \cdot\left\{\exp\left\{\left(j\omega\sqrt{LC}\right)(w_0/2) - x/w_0\right\}^2\right. \\ & \cdot\left\{1-\operatorname{erf}\left[\left(j\omega\sqrt{LC}\right)(w_0/2) - x/w_0\right]\right\} \\ & -\exp\left\{\left(j\omega\sqrt{LC}\right)(w_0/2) + x/\omega_0\right\}^2 \\ & \left.\cdot\left\{1-\operatorname{erf}\left[\left(j\omega\sqrt{LC}\right)(w_0/2) + x/\omega_0\right]\right\}\right\}. \end{aligned} \tag{26}$$

The product $\omega\sqrt{LC} = k_e$ is simply the propagation constant of the microstrip line, and $k_e = k\sqrt{\epsilon_e}$, where ϵ_e is the effective relative dielectric constant of the microstrip line. Making this substitution, we find that (26) can be expressed as the sum of a forward-traveling voltage wave $v^+(x)$ and a reverse-traveling wave $v^-(x)$, so that $v(x) = v^+(x) + v^-(x)$ where

$$v^+(x) = \frac{v_3 F w_0\sqrt{\pi}}{2}\left[1-\operatorname{erf}\left(jk_e w_0/2 - x/w_0\right)\right] \cdot\exp\left(-\frac{k_e^2 w_0^2}{4}\right)e^{-jk_e x} \tag{27}$$

$$v^-(x) = \frac{-v_3 F w_0\sqrt{\pi}}{2}\left[1-\operatorname{erf}\left(jk_e w_0/2 - x/w_0\right)\right] \cdot\exp\left(-\frac{k_e^2 w_0^2}{4}\right)e^{+jk_e x}. \tag{28}$$

Suppose the infinite microstrip is now terminated in matched loads at port 1 ($x = x_1$) and port 2 ($x = x_2$), as shown in Fig. 4. The voltage v_2 at port 2 results from the forward-traveling wave arriving at x_2, which is different from the voltage $v^+(x_2)$ of the infinite line because of the missing contribution from the omitted part of the line extending from $x = -\infty$ to $x = x_1$. This missing contribution in Fig. 4(b) is simply $v^+(x_1)$ times the phase factor $e^{-jk_e(x_2-x_1)}$, leading to this expression for the net voltage $v_2(x_2)$ of the finite line:

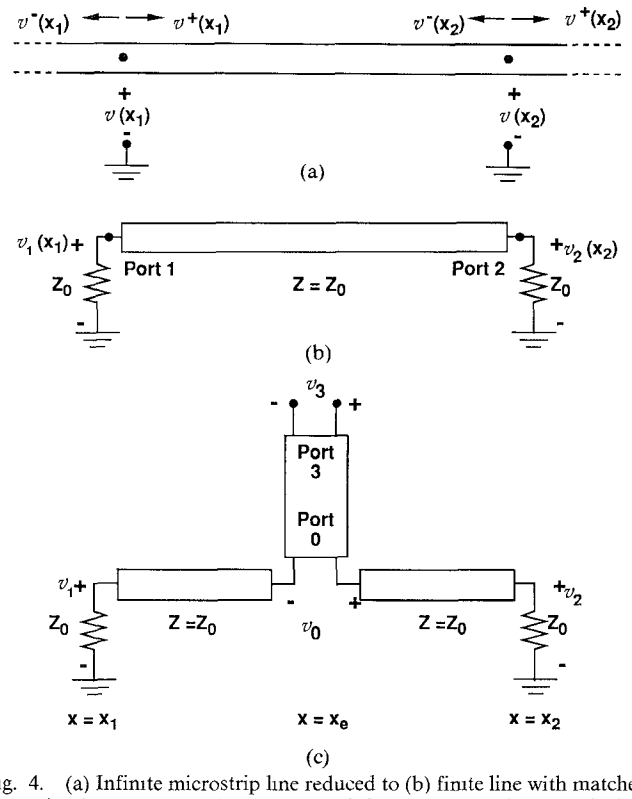

Fig. 4. (a) Infinite microstrip line reduced to (b) finite line with matched terminations at ports 1 ($x = x_1$) and 2 ($x = x_2$), and (c) equivalent circuit showing line broken at $x = x_e$ and fed by port 0 of two-port.

$$v_2(x_2) = v^+(x_2) - v^+(x_1)e^{-jk_e(x_2-x_1)}. \tag{29}$$

A similar argument gives

$$v_1(x_1) = v^-(x_1) - v^-(x_2)e^{-jk_e(x_2-x_1)}. \tag{30}$$

When these differences are evaluated the error function integrations in the complex plane cancel over most of their extent, leaving

$$v_2(x_2) = \frac{v_3 F}{2k_e}(I_R + jI_I)e^{-jk_e x_2} \tag{31}$$

and

$$v_1(x_1) = \frac{-v_3 F}{2k_e}(I_R - jI_I)e^{+jk_e x_1} \tag{32}$$

in which the integrals I_R and I_I are defined in terms of normalized coordinates $u_1 = k_e x_1$, $u_2 = k_e x_2$ and a normalized beam radius $\gamma_0 = k_e w_0$:

$$I_R \equiv \int_{u_1}^{u_2}\cos(u)e^{-u^2/\gamma_0^2}\,du \tag{33}$$

$$I_I \equiv \int_{u_1}^{u_2}\sin(u)e^{-u^2/\gamma_0^2}\,du. \tag{34}$$

To complete the analysis we must determine the Q value of the resonant mode which determines the complex-valued resonant frequency ω_0 in terms of Q and

ω_r [7]:

$$\omega_0^2 = \omega_r^2\left(1+\frac{j}{Q}\right). \tag{35}$$

The value of Q, assuming no wall or diffraction losses for the moment, can be found by taking the ratio of stored energy U to energy dissipated in the microstrip loads per cycle at resonance. This is most easily done by letting $\vec{H} = \vec{H}_0$, since our choice of normalization then gives a numerical value for U of $\frac{1}{2}$. Using the expressions for $v_1(x_1)$ and $v_2(x_2)$ to find total average power $P_d = (|v_1|^2 + |v_2|^2)/2Z_0$, we obtain after some algebra:

$$Q = \frac{\pi}{2}\frac{Z_0}{\omega_r\mu_0 h}\frac{G}{h}k_e^2 w_0^2\frac{(k_d h)^2}{\sin^2(k_d h)}\frac{e^{2y_0^2/w_0^2}}{(I_R^2+I_I^2)}. \tag{36}$$

Substitution of this Q value into (35) now completes the expression for $F(\omega)$ and determines v_1 and v_2 in relation to the driving voltage v_3.

D. Resonator Equivalent Circuit

Let us now derive an equivalent circuit for the case illustrated in Fig. 3. Examination of the form of the voltages v_1 and v_2 in (31) and (32) shows that they are equal in magnitude and differ in phase by a factor related to position. This suggests an equivalent circuit of the form shown in Fig. 4(c), in which both v_1 and v_2 arise from a voltage v_0 at port 0 of a hypothetical two-port. The new voltage v_0 is related to v_1 and v_2 by

$$v_1 = \frac{-v_0}{2}e^{-jk_e(x_e-x_1)} \tag{37}$$

$$v_2 = \frac{+v_0}{2}e^{-jk_e(x_2-x_e)} \tag{38}$$

and if we define the location of the equivalent port to be x_e, we find that

$$x_e = \frac{1}{k_e}\left[\arctan\left(\frac{I_I}{I_R}\right)+\pi n\right] \tag{39}$$

where n is an integer chosen such that $x_1 < x_e < x_2$. The expression for v_0 that gives the desired forms of v_1 and v_2 is now

$$v_0 = \frac{(I_R^2+I_I^2)^{1/2}F(\omega)}{k_e}v_3 \equiv h_{03}v_3 \tag{40}$$

in which we have introduced the dimensionless hybrid parameter h_{03}. Since the load viewed from port 0 is simply $2Z_0$, the problem of simulating a three-port circuit terminated in Z_0 at ports 1 and 2 has been reduced to the problem of simulating a two-port circuit with a load $2Z_0$ at port 0.

Since by assumption the resonator is lossless, its two-port admittance matrix is composed of four purely imaginary elements. By reciprocity, two of these elements are equal ($Y_{03} = Y_{30}$), so there are only three independent variables to be determined: Y_{00}, $Y_{03} = Y_{30}$, and Y_{33}. The behavior of these parameters near resonance can be found by conserving complex power. Let $\mathscr{P}$ be the complex power entering port 3. Then if P_d is the (real) power dissipated at the load $2Z_0$ on port 0, and W_m and W_e denote the average stored magnetic- and electric-field energies respectively, complex power is [9]

$$\mathscr{P} = P_d + j2\omega(W_m - W_e) = \frac{|v_3|^2 Y_{in}^*}{2} \tag{41}$$

where Y_{in} is the input admittance at port 3 when port 0 is terminated in $2Z_0$. Near the resonant frequency $\omega = \omega_r$, the real part G_{in} of Y_{in} will be stationary with respect to frequency and Y_{in} can be approximated by

$$Y_{in} \approx G_{in} + j\Delta\omega\left.\frac{\partial B_{in}}{\partial\omega}\right|_{\omega=\omega_r} \tag{42}$$

where $Y_{in} = G_{in} + jB_{in}$ and $\Delta\omega = \omega - \omega_r$. At resonance ($\Delta\omega = 0$), the complex power $\mathscr{P}$ becomes purely real and must equal the power P_d dissipated in port 0's load. Relating v_0 to v_3 via (40) for $\omega = \omega_r$ gives

$$G_{in} = \frac{4}{\pi}\cdot\frac{Qs^2\cos^2(k_d h)\exp(-2\rho_3^2/w_0^2)}{\omega_r\mu_0 G w_0^2}. \tag{43}$$

The value of $\partial B_{in}/\partial\omega$ can be found by differentiating (41) with respect to ω and recognizing that $W_m = W_e$ at resonance. This gives

$$-\frac{4\omega_r}{|v_3|^2}\frac{\partial}{\partial\omega}(W_m - W_e) = \frac{\partial B_{in}}{\partial\omega}. \tag{44}$$

The frequency dependence of the stored-energy terms comes from the mode expansion of the fields, which results in these expressions for W_m and W_e in terms of Q, P_d, ω_0, and ω_r:

$$W_m = \left|\frac{j\omega}{\omega^2-\omega_0^2}\right|^2\frac{P_d\omega_r}{Q} \tag{45}$$

$$W_e = \left|\frac{j\omega_0}{\omega^2-\omega_0^2}\right|^2\frac{P_d\omega_r}{\left(Q+\frac{1}{2Q}\right)}. \tag{46}$$

At $\omega = \omega_r$, W_e is stationary and (45) substituted into (44) gives

$$\frac{\partial B_{in}}{\partial\omega} = -\frac{2Q}{\omega_r}G_{in}. \tag{47}$$

Now that Y_{in} and h_{03} have been found, all that remains is to devise an equivalent circuit whose Y_{in} and h_{03} equal those of the physical system when both are loaded by $2Z_0$ at port 0. It is a straightforward matter to show that if the three real quantities G_{in}, B_{in}, and $|h_{03}|$ correspond, then so must the imaginary values Y_{00}, Y_{03}, and Y_{33}. Hence the circuit devised will be truly equivalent in the neighborhood of resonance.

Consider the lumped-element equivalent circuit in Fig. 5 which we choose to model the two-port block in Fig. 4(c). Suppose the series capacitance C_F is much smaller than

C_0. Far from resonance, the admittance at port 3 will approach $j\omega C_F$. Since this behavior is shown by the open-circuit microstrip of Fig. 3, we choose to set C_F equal to this fringing capacitance. Derneryd [6] gives an approximate expression for C_F in terms of h, s, ϵ_e, and line impedance Z_0:

$$C_F = \frac{0.412h\sqrt{\epsilon_e\epsilon_0\mu_0}}{Z_0}\cdot\frac{\epsilon_e+0.3}{\epsilon_e-0.258}\cdot\frac{s/h+0.262}{s/h+0.813}. \quad (48)$$

For practical microstrips C_F is typically less than 0.1 pF.

We will now show how C_0, L_0 and N can be selected so as to model the behavior of the open resonator-microstrip circuit in the neighborhood of resonance. First we require that the input admittance $Y_e = G_e + jB_e$ is real at the resonant frequency ω_r. Let $R = 2N^2Z_0$ be the resistance across the tank circuit reflected through the ideal transformer. If Y_e is real at $\omega = \omega_r$, then L_0 and C_0 must satisfy

$$\left(\frac{\omega_r L_0}{R}\right)^2 = \left[\omega_r^2 L_0(C_0+C_F)-1\right]\left[1-\omega_r^2 L_0 C_0\right]. \quad (49)$$

At resonance, it can be shown that

$$\mathrm{Re}(Y_e) = \left\{\frac{R}{2}+\left[\frac{R^2}{4}+\frac{1}{(\omega_r C_F)^2}\right]^{1/2}\right\}^{-1} = G_{in}. \quad (50)$$

Setting $\mathrm{Re}(Y_e) = G_{in}$ determines R and thus N, since Z_0 is fixed. This insures the equivalence of h_{03} and G_{in}. The expression for $\partial B_e/\partial\omega$ is quite complicated, but for $Q_e = \omega L_0/R$ greater than 100, this approximation is correct to within 0.2 percent:

$$\frac{\partial B_e}{\partial\omega} \approx \frac{-2C_F^2R^2}{L_0} = \frac{\partial B_{in}}{\partial\omega}. \quad (51)$$

Eq. (51) determines L_0, which can be used in (49) to find C_0 exactly. Thus all three parameters of the equivalent circuit N, L_0, and C_0 have been found in terms of the open resonator parameters. When the values for G_{in} and $\partial B_{in}/\partial\omega$ found from the open resonator are used in (50) and (51), we obtain these explicit expressions for the equivalent circuit component values:

$$N = \left\{\frac{1}{2Z_0}\left[\frac{1}{G_{in}}+\frac{G_{in}}{(\omega_r C_F)^2}\right]\right\}^{1/2} \quad (52)$$

$$L_0 = \frac{4C_F^2N^4Z_0^2\omega_r}{QG_{in}} \quad (53)$$

$$C_0 = C_F\left[\omega_r^{-2}\left(L_0C_F - L_0^2/R^2\right)^{-1}-1\right]. \quad (54)$$

III. Experiments

A. Applicability of the Theory

It is optimistic to expect the simplified analytical expressions derived above to model exactly the very complex microstrip open resonator system. Our theory is incomplete in that we have not attempted to solve Maxwell's equations self-consistently. Instead, we began with a solution for the more tractable case of a bare dielectric slab in an open resonator, and assumed these fields were undisturbed by the insertion of microstrip lines. Up to now we have also neglected all mechanisms of energy loss other than the power coupled out of the resonator by the microstrip lines. In the following section we will show how the equivalent circuit of Fig. 5 may be modified by adding an empirically derived resistor R_0 to model diffraction and ohmic losses. The microstrip lines also perturb the resonant frequency ω_r away from the value predicted from the bare-slab analysis, so in the following analyses ω_r is determined by experiment. With these empirical corrections we will show that the theory predicts experimental Q values to within a factor of two or better. More sophisticated analyses will no doubt improve this accuracy, but the goal of achieving a semiquantitative understanding of the coupling between microstrip lines and an open resonator has been achieved.

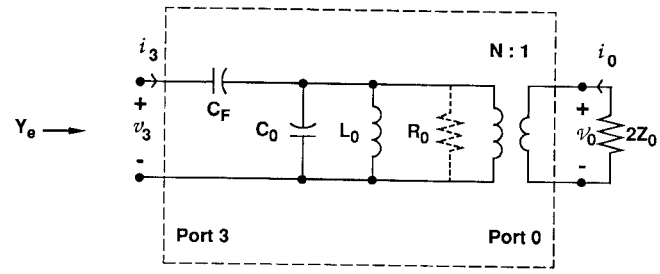

Fig. 5. Equivalent circuit for two-port block of Fig. 4(c).

B. Diffraction and Ohmic Losses

Diffraction losses *per se* in an empty open resonator can be very low, as Beyer and Schiebe showed in their experimental study of open resonators at 9 GHz [10]. However, when any metallic object such as a microstrip line is placed within the open resonator fields, induced currents on the object radiate power out of the resonator. This extrinsic diffraction loss or scattering loss was studied experimentally by constructing an open resonator along the lines of Figs. 1 and 2. In all the experiments to be described, we used a polished, gold-plated, aluminum spherical reflector whose radius of curvature $R = 156.2$ mm was equal to its usable diameter. The flat reflector was a brass plate approximately 15 cm square mounted on a motor-driven translation stage so that the inter-reflector distance D could be adjusted with a resolution of 2.5 μm. The coaxial-loop coupling method of Beyer and Schiebe [10] was used to measure the unloaded quality factor Q_0.

To investigate the scattering effects of microstrip lines on the Q_0 of an open resonator mode, we first tracked the Q_0 of the TEM_{003} mode of the empty resonator as a function of D to establish a baseline. This baseline value is established by a combination of diffraction losses and ohmic losses. The latter can be predicted from theory [11] and for this resonator the Q_0 calculated from ohmic losses alone is $D/(S_b+S_g)$, in which the skin depths for brass

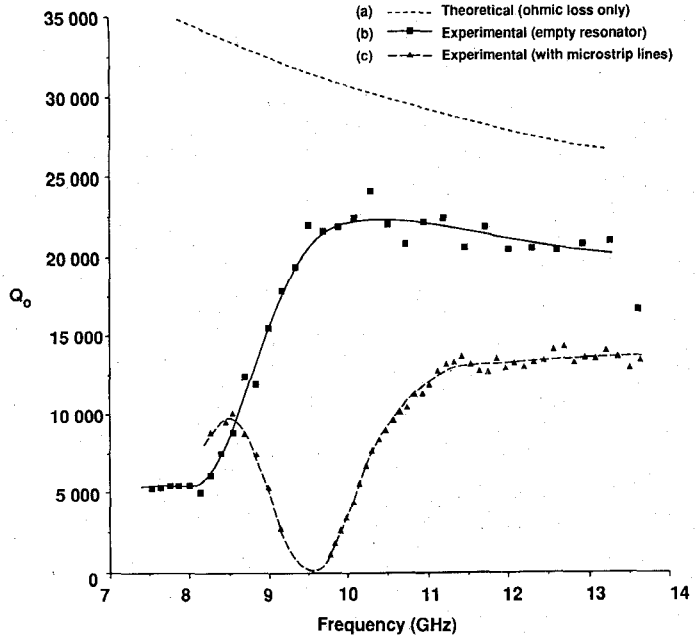

Fig. 6. Unloaded Q of TEM_{003} mode versus frequency as inter-reflector distance D is varied. (a) Theoretical maximum Q_0 including ohmic loss only. (b) Measured Q_0 of empty resonator. (c) Measured Q_0 of resonator with substrate and microstrip lines.

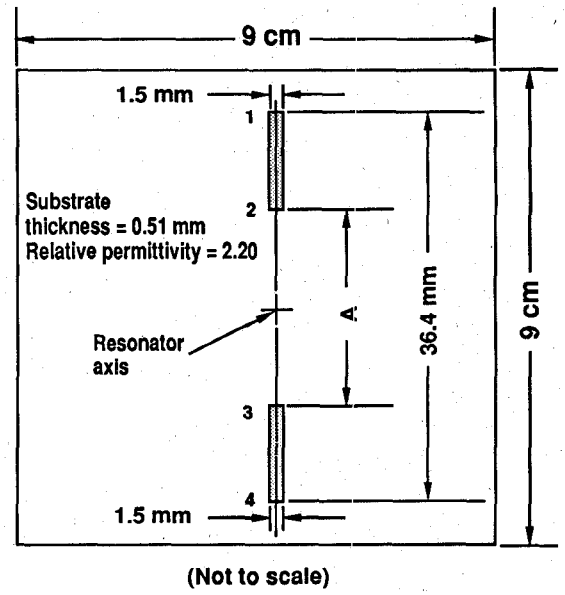

Fig. 7. Dimensions of dielectric substrate and microstrip lines mounted on flat reflector of open resonator (distance A given in text).

(S_b) and gold (S_g) are found using conductivities of $1.57 \cdot 10^7$ S/M and $4.1 \cdot 10^7$ S/M respectively.

In Fig. 6 the experimental values for Q_0 are plotted for the TEM_{003} mode as a function of resonant frequency. The parameter D was varied from 46.5 mm to 84.6 mm to obtain the frequency range illustrated. Above 10 GHz, the measured data for the empty resonator follow the shape of the theoretical ohmic-loss limit, although differing from it by a constant scale factor probably caused by surface roughness, which increases the ohmic loss above its theoretical value. Below 10 GHz, the experimental empty resonator Q_0 falls rapidly because of diffraction from the edge of the spherical reflector, where the beam intensity is only 11.6 dB below its on-axis value at 9 GHz.

A dielectric substrate with two microstrip lines having the dimensions shown in Fig. 7 ($A = 14.6$ mm) was mounted on the flat reflector, with due precautions taken to insure the flatness of the ground plane. The width of the microstrips was chosen so that their characteristic impedance was 50 ohms. The measurements of Q_0 versus distance were then repeated. Above 11 GHz, the quality factor fell from about 20,000 to about 13,500 but showed no strong frequency dependence. This decrease can be attributed to a combination of dielectric substrate losses (expected to be comparatively small in this case) and nonresonant scattering from the microstrip lines. Near 9.8 GHz the open-ended lines are a half-wave long electrically, so their resonant scattering cross-section increases greatly above its nonresonant value. This effect is demonstrated by the sharp drop in Q_0 for this case, with a minimum value below measurable limits at about 9.6 GHz. A modified version of this experiment has been used to measure the scattering cross-section of symmetrical objects such as wires [12]. When the microstrips are terminated in a resistive load, as in the next section's experiments, they cease to be resonant lines, and scattering decreases so that reasonably high Q values are once again obtainable.

C. Open-Resonator-Coupled Microstrip Lines

In these experiments the same configuration of microstrip lines as in Fig. 7 was used. Two 0.9 mm O.D. 50 ohm coaxial cables were brought through the flat reflector to ports 1 and 4 of the microstrip lines. The cable's shield was soldered to the back of the microstrip ground plane and its center conductor extended through a small hole in the substrate to join the end of the microstrip line. Since the coaxial line loss of about 2 dB was not a part of the intrinsic loss of the system, it has been subtracted from the raw experimental loss data. Reflections from the imperfect coaxial–microstrip transitions limited the accuracy of the transmission loss measurements to about ± 0.4 dB.

Three physical configurations of the microstrip lines were examined. In the first configuration, the spacing A was 26.9 mm, which meant that the lines were electrically short and coupling was mediated primarily by the fringing electric field at the open-circuited ports 2 and 3. We will denote this case (a) as electric coupling, although some voltage was induced by the magnetic field in the short microstrip sections and both effects were included in the equivalent circuit model. The second configuration was obtained from the first by adding symmetrically placed short-circuited stubs at ports 1 and 4. This had the effect of placing shunt inductances (calculated total value $L = 0.637$ nH) across these ports, which tuned out some of the capacitive susceptance shown by these electrically short lines. This second case (b) we term electric coupling with matching. Finally, the inductive stubs were removed and a circuit having a distance of $A = 14.6$ mm was studied. The

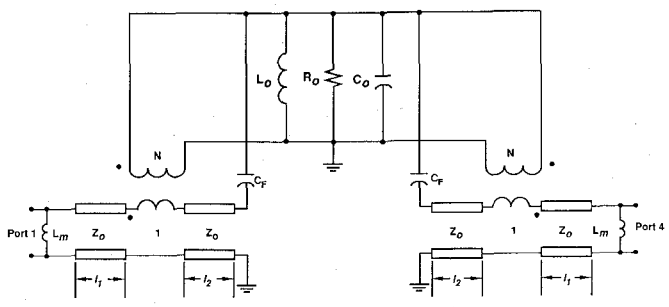

Fig. 8. General equivalent circuit for microstrip lines coupled via open resonator mode.

longer microstrip lines of this third case coupled substantially to both the electric and the magnetic fields, so we refer to this case (c) as electromagnetic coupling.

Equivalent circuit models for these cases were obtained by extending the conceptual three-port circuit of Figs. 4(c) and 5 in a straightforward manner. Empirically determined values for unloaded resonator Q_0 due solely to scattering and ohmic losses were modeled by inserting a resistor of value $R_0 = \omega_r L_0 Q_0$ into the equivalent circuit of Fig. 5. The resulting equivalent circuit for all three cases is shown in Fig. 8. All component values with the exception of C_0 and R_0 were calculated from first principles using the theory of Section II. The transmission loss in a 50 ohm system from port 1 to port 4 was then measured for all three cases. A typical response showed a peak in $|S_{41}|$ at the mode's resonant frequency ω_r with a maximum value $|S_{41}|_{\max}$ and a 3 dB radian frequency bandwidth $\Delta\omega$ from which an experimental value for the loaded quality factor $Q_l = \omega_r/\Delta\omega$ was obtained.

In order to compare the experiments with theory, the remaining component values C_0 and R_0 must be established. Taking the frequency at which $|S_{41}|_{\max}$ occurs to be the experimental resonant frequency, we used this value of ω_r in (54) to find C_0. Since no independent measurements of Q_0 were made, we chose to adjust R_0's value empirically until the equivalent circuit's $|S_{41}|_{\max}$ agreed with the experimental value. The values for all components of Fig. 8 are given in Table I.

Because the values of minimum insertion loss $|S_{41}|_{\max}$ were forced to agree in order to determine R_0, the predictive power of the theory cannot be judged by comparing $|S_{41}|_{\max}$ of the equivalent circuits and the experiments. Instead, comparing the experimental values of Q_l to those obtained from the frequency responses calculated for the equivalent circuits will reveal how accurately the model simulates the experiments.

This comparison is shown in Table II. In each case the TEM_{002} mode was excited. For the configuration chosen, the electric coupling of case (a) was fairly loose, resulting in a relatively high minimum loss of 3.8 dB. However, this light loading led to a relatively high loaded Q_l value of 3000. The inductive stubs of case (b) improved the impedance match to the 50 ohm measurement system and lowered the minimum loss to only 1.3 dB. The corresponding loaded Q_l fell to a still respectable value of 1200. The

TABLE I
EQUIVALENT CIRCUIT VALUES

Case	C_F	C_0	L_0	L_m	ℓ_1	ℓ_2	N	R_0
(a) Electric coupling	11.6 fF	12.5554 pF	21.1719 pH	∞	2.46 mm	0	13.675	6,600 ohms
(b) Electric coupling w/matching	11.6 fF	12.530 pF	20.1557 pH	0.637 nH	2.46 mm	2.28 mm	13.096	13,300 ohms
(c) Electro-magnetic coupling	11.6 fF	8.28693 pF	30.4767 pH	∞	5.88 mm	5.00 mm	8.817	11,800 ohms

TABLE II
EXPERIMENTAL DATA

Case	D (cm)	Resonant Frequency (GHz)	Measured* $\lvert S_{41}\rvert_{\max}$ (dB $\pm$ 0.4 dB)	Measured Q_l	Equivalent Circuit Q_l
(a) Electric coupling	4.95	9.751	3.8	3000	1780
(b) Electric coupling w/matching	4.79	10.006	1.3	1200	1470
(c) Electromagnetic coupling	4.79	10.00	0.8	860	540

greatest amount of coupling was obtained in case (c), in which the electric fringing-field coupling combined with magnetic coupling to give a minimum loss of only 0.8 dB, with an accompanying Q_l of 860. Although higher Q_l values can be obtained at 10 GHz with dielectric resonators, the virtue of these cases lies in the fact that scaling an open resonator system upward in frequency makes it more convenient, not less. Also, diffraction-limited Q values should remain approximately constant with scaling, so that the same circuit scaled to the millimeter wave range will show a Q that is degraded only by the higher skin-effect losses at those frequencies.

Comparing the experimental values for Q_l with the theoretical equivalent circuit values, the models for (a) electric and (c) electromagnetic coupling predict a Q_l about 40 percent lower than those found experimentally. The case (b) of electric coupling with matching was about 20 percent higher. We have somewhat artificially separated the coupling into a purely magnetic part along the microstrip and a purely electric part at the open ends, whereas the actual situation is considerably different. Both the electric and magnetic fields couple energy all along the microstrip, and the true electric field in particular is quite different than it is in the dielectric-only case which we have used in the theory. Nevertheless, trends are predicted well, and the rather elementary theory we have presented can serve as a guide for future theoretical and experimental work in this area.

IV. CONCLUSIONS

The application of open-resonator coupling techniques to millimeter wave circuit design has the potential for improving any circuit in which a high Q element is needed. Filter design is an obvious use, since the circuit we studied is essentially a one-pole bandpass filter. Even if the cavity Q is limited by ohmic losses, the Q_0 of a 100 GHz cavity formed with a 1.56 cm spherical reflector can be expected to reach about 7800, which is quite attractive when obtained from a resonator not much larger than typical waveguide components at these frequencies. A two-pole

filter could be achieved in one resonator structure by utilizing orthogonally polarized TEM modes.

In a related experiment [13] the authors have demonstrated that a single microstrip couples to an open resonator mode in a manner similar to a dielectric resonator, and so can be used for reflection stabilization of oscillators [14], in which a combined output power of 13.3 mW was obtained from two *X* band microstrip Gunn oscillators whose individual power outputs obtained through purely planar techniques never exceeded 3 mW each. The demonstration of such improvements indicates that the open resonator has a promising future as an adjunct to conventional millimeter wave planar circuits.

ACKNOWLEDGMENT

Thanks are extended to Robert W. Jackson and the reviewers for helpful criticisms and comments.

REFERENCES

[1] K. C. Gupta, R. Garg, and I. J. Bahl, *Microstrip Lines and Slotlines*. Norwood, MA: Artech House, 1979, pp. 93–95.
[2] H. Kogelnik and T. Li, "Laser beams and resonators," *Proc. IEEE*, vol. 54, pp. 1312–1328, Oct. 1966.
[3] A. E. Siegman, *An Introduction to Lasers and Masers*. New York: McGraw–Hill, 1971, pp. 293–345.
[4] J. W. Mink, "Quasi-optical power combining of solid-state millimeter-wave sources," *IEEE Trans. Microwave Theory Tech.*, vol. MTT-34, pp. 273–279, Feb. 1986.
[5] A. L. Cullen, "Millimeter-wave open-resonator techniques," in *Infrared and Millimeter Waves*, vol. 4. New York: Academic Press, 1983.
[6] A. G. Derneryd, "Linearly polarized microstrip antennas," *IEEE Trans. Antennas Propagat.*, vol. AP-24, pp. 846–851, Nov. 1976.
[7] R. F. Harrington, *Time-Harmonic Electromagnetic Fields*. New York: McGraw–Hill, 1961, pp. 431–434.
[8] I. N. Sneddon, *Fourier Transforms*. New York: McGraw–Hill, 1951, pp. 230–231.
[9] R. F. Harrington, *Time-Harmonic Electromagnetic Fields*. New York: McGraw–Hill, 1961, p. 22.
[10] J. B. Beyer and E. H. Schiebe, "Loss measurements of the beam waveguide," *IEEE Trans. Microwave Theory Tech.*, vol. MTT-11, pp. 18–22, Jan. 1963.
[11] R. G. Jones, "Precise dielectric constant measurements at 35 GHz using an open microwave resonator," *Proc. Inst. Elec. Eng.* vol. 123, pp. 385–390, Apr. 1976.
[12] C. M. Tang and A. L. Cullen, "Determination of scattering widths of a long thin wire using an open resonator," *Elec. Ltrs.*, vol. 14, pp. 245–246, Apr. 1978.
[13] K. D. Stephan, S. L. Young, and S. C. Wong, "Open cavity resonator as high-*Q* microstrip circuit element," *Elec. Ltrs.*, vol. 23, pp. 1028–1029, Sept. 1987; also see *Erratum*, v. 23, p. 1397, Dec. 1987.
[14] S. L. Young and K. D. Stephan, "Stabilization and power combining of planar microwave oscillators using an open resonator," in *1987 IEEE Int. Microwave Symp. Dig.* (Las Vegas, NV), pp. 185–188.

Karl D. Stephan (S'81–M'83) received the B.S. degree in engineering from the California Institute of Technology, Pasadena, in 1976, and the M. Eng. degree from Cornell University, Ithaca NY, in 1977. He received the Ph.D. degree in electrical engineering from the University of Texas at Austin in 1983.

In 1977, he joined Motorola, Inc. From 1979 to 1981 he was with Scientific-Atlanta, where he engaged in research and development pertaining to cable television systems. In September, 1983, he joined the faculty of the University of Massachusetts at Amherst, where he is presently Assistant Professor of Electrical Engineering. His current research interests include the application of quasi-optical techniques to millimeter wave circuits and subsystems.

✠

Song-Lin Young was born in Chang-Hwa, Taiwan, Republic of China, on April 18, 1961. From 1983 to 1985, he served as a field service officer in the radar corps of the Taiwanese Navy. He has been with the Department of Electrical and Computer Engineering, University of Massachusetts at Amherst since 1986 and is currently working toward his M.S. degree. His graduate study at the University of Massachusetts involves coupled microwave and millimeter-wave oscillators for applications in phased arrays and quasi-optical power combining systems.

✠

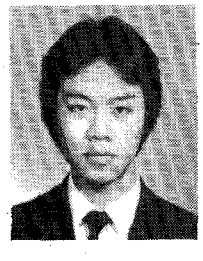

Sai-Chu Wong was born in Hong Kong on December 14, 1964. He received the B.Sc. degree in electrical engineering from the University of Massachusetts at Amherst in 1988.

In 1987 he joined the Laboratory for Millimeter Devices and Applications, University of Massachusetts, where he is presently involved in the research of quasi-optical permittivity measurement of thin uniaxial and biaxial films.